Techno-Economic Analysis of Fuel Switching from Coal to Natural Gas for NPK Fertilizer Drying Process

Devi Intan Silviani, Rakhma Ayu Giarti, Daril Ridho Zuchrillah, Rizal Arifin*

Industrial Chemical Engineering, Faculty of Vocational Studies, Institut Teknologi Sepuluh Nopember, Kampus Sukolilo, Jl. Raya ITS, Surabaya, 60111, Indonesia
**Corresponding author: rizal.arifin@its.ac.id*

Abstract
Using coal as the primary fuel in the NPK fertilizer industry contributes significantly to carbon dioxide (CO_2) emissions, which negatively impact the environment and hinder the achievement of national decarbonization targets. To address this, this project aims to evaluate the technical and economic feasibility of switching from coal to natural gas in the furnace unit of the NPK fertilizer production process. As demands for efficiency and sustainability increase, the evaluation of fuel switching to natural gas is underway. This study re-simulates the combustion process in the furnace using Aspen Plus V14. Evaluation is carried out on thermal performance, CO_2 emissions, and economic indicators, including Capital Expenditure, Operational Expenditure, NPV, IRR, and Payback Period. The results show that natural gas achieves a thermal efficiency of 90.11% and reduces direct furnace CO_2 emissions by 27.5% compared with coal. However, implementation requires replacement of the combustion system and installation of configuration-specific auxiliary equipment and piping, resulting in an incremental investment of USD 72,120.17. The natural-gas configuration also increases annual OpEx by USD 12,594.33, primarily because of its higher fuel cost. Under the base-case incremental replacement and carbon-value assumptions, the project yields an NPV of USD 76,557.28, an IRR of 32.10%, a simple payback period of 3.04 years, and a discounted payback period of 4.01 years. Without monetization of the direct CO_2 reduction, the NPV decreases to −USD 128,543.85. Therefore, fuel switching provides technical and direct-emission benefits, but its economic feasibility is conditional on the assumed carbon value, fuel prices, and eligibility of the emission reduction for monetization.

Keywords: Carbon Emissions; Coal; Decarbonization; Economic Analysis; Fuel Switching.

1. Introduction

The current global dynamics, particularly those related to geopolitical issues, have caused a worldwide crisis affecting the energy sector. This situation is believed to have increased international awareness of the importance of energy and national economic security, leading several countries to shift energy policies toward strengthening domestic capabilities. According to data from the past five years, fossil fuels, including oil, gas, and coal, continue to dominate and play a vital role in Indonesia's energy supply [1].

Granulated NPK fertilizer production involves several downstream operations, including granulation, drying, screening, cooling, and coating. The drying unit is particularly relevant because wet granules leaving the granulator must be conditioned to the required final moisture content using a continuous supply of thermal energy. An evaluation of an Indonesian NPK steam-granulation plant reported that the rotary dryer reduced granule moisture from approximately 4% to below 1.5% and identified the dryer as one of the main process units [2]. In the plant evaluated in this study, the furnace provides the thermal energy required to produce the hot drying air. Consequently, switching the furnace fuel directly affects heat-supply performance, onsite CO_2 emissions, and operating costs, while the upstream NPK formulation and granulation stages remain outside the modification boundary. This direct coupling makes the furnace–dryer subsystem a well-defined and industrially relevant case for evaluating brownfield fuel switching. Alternative decarbonization pathways include post-combustion carbon capture, utilization, and storage; however, their economic feasibility remains a major implementation constraint [3], [4].

Using coal as an energy source in Indonesia faces several significant environmental, economic, and regulatory sustainability challenges. The main challenge relates to the ecological impact of coal combustion, which produces greenhouse gas emissions, particularly CO_2, which is a major contributor to climate change [5]. Coal combustion

Received: Apr 08, 2026
Accepted: July 18, 2026
DOI: 10.12962/j28075064.v12i1.a9573

produces significant amounts of CO_2 emissions and fly ash, which can lead to unhealthy environmental conditions [6]. Besides CO_2, coal combustion emits other pollutants such as sulfur dioxide (SOx) and nitrogen oxides (NOx), which negatively impact air quality and public health [7], [8].

The following sustainability challenge is the development of regulations at both the national and international levels that require reductions in carbon emissions and environmental pollution. Indonesia, through its Nationally Determined Contribution (NDC), initially aimed for a 29% reduction in emissions under business-as-usual (BAU) scenarios and a 41% reduction with conditions (with adequate international support) by 2030 [9]. This commitment indirectly binds and compels the government and industry to seek innovative solutions to reduce emissions from coal-fired energy sources. This includes an energy transition supported by policies like the National Energy General Plan (RUEN), which aims for 23% renewable energy in the national energy mix by 2025 and 31% by 2050. Beyond the environmental and regulatory challenges, sustainability challenges also arise from an economic perspective, where the implementation of carbon pricing policies continues to increase alongside rising energy demand. Therefore, these sustainability challenges are expected to encourage the industry to reduce its reliance on coal and shift to cleaner energy sources, including natural gas.

As an energy source, natural gas has the third-largest reserves in the world after coal and petroleum. In Indonesia, the role of natural gas as an energy source is becoming increasingly significant, aligning with policies aimed at reducing the reliance on oil as the primary energy source. This transition is supported by the government's commitment to the Clean Development Mechanism (CDM) under the Kyoto Protocol, in which natural gas is chosen as a more environmentally friendly alternative because it produces lower pollution [10]. Its advantage as an energy source lies in its lower carbon emissions, capable of reducing CO_2 emissions by up to 25% compared to other fossil fuels. Additionally, natural-gas combustion generally produces fewer particulate emissions than coal combustion [11]. However, the presence and environmental implications of sulfur compounds depend on the delivered-gas specification and any upstream gas-treatment processes [4], [12]. From an economic perspective, using natural gas is also more advantageous in the long term because its price is relatively stable and tends to be more economical than that of other fossil fuels. With these various advantages, natural gas has become one of the leading solutions in supporting the energy transition towards a more sustainable system [6].

Based on previous research, efforts to reduce carbon dioxide (CO_2) emissions from coal combustion show that PtG offers an effective solution to this problem by converting CO_2 emissions into energy [13]. The system used involves carbon capture, electrolysis, and methanation. The estimated emission reduction from this measure is from 62.5 million tons to 28.15 million tons. Recent assessments of industrial boilers and furnaces have shown that switching from conventional liquid or solid fuels to natural gas can reduce direct emissions and improve thermal performance, although the economic outcome remains dependent on fuel prices and equipment-modification requirements [14], [15].

However, switching from coal to natural gas requires significant investment and operational changes, so economic analysis is crucial to determine whether the investment is feasible. This analysis must consider initial investment costs, operational costs, fluctuating fuel prices, and potential return on investment. Additionally, switching value analysis is necessary due to changes in the flow of benefits and costs. These results will assist decision-makers in determining whether fuel switching is financially and economically viable [16].

Previous studies have generally evaluated coal-to-natural-gas switching at the power-generation or national energy-system level, whereas plant-specific assessments for thermal operations in fertilizer production remain limited. This study contributes by integrating a site-specific Aspen Plus combustion model with an incremental techno-economic evaluation of replacing an existing coal-fired furnace with a natural-gas-fired system for an NPK fertilizer rotary dryer. The analysis simultaneously compares direct combustion emissions, thermal performance, capital requirements, operating-cost changes, and discounted-cash-flow indicators. The results therefore provide a case-specific decision basis for brownfield fuel switching in the Indonesian fertilizer industry.

Nomenclature

ARE	absolute relative error
CEPCI	chemical engineering plant cost index
η_{th}	thermal efficiency

$net\ Q_{generated}$	net heat transferred to the drying-air stream
$\dot{m}_{fuel}$	fuel mass flow-rate
HV_{fuel}	fuel heating value
Y_{sim}	simulation result
Y_{plant}	plant operating value
GJ	gigajoule
adb	air-dried basis
wt	percent by weight
daf	dry ash free
Q	heat

2. Methodology

2.1 Feed Specifications

In this research, coal and natural gas are considered as raw materials for modeling combustion systems. Each fuel was characterized to support simulation accuracy and facilitate evaluation of its thermal performance. Based on the plant fuel specification, the coal was classified as sub-bituminous coal. In the Aspen Plus simulation environment, coal is categorized as a non-conventional solid. Therefore, analyzing the coal, including its proximate, ultimate, and sulfur analysis data, is necessary to estimate its characteristics [17].

Ultimate analysis, presented in Table 2, is used to determine the content of the main elements in coal, such as carbon (C), hydrogen (H), nitrogen (N), sulfur (S), chlorine (Cl), and oxygen (O). Meanwhile, proximate analysis, as shown in Table 1, provides data on the overall components of coal, namely moisture, volatile matter, fixed carbon, and ash. Sulfur analysis, depicted in Table 3, is also conducted to determine the distribution of sulfur content in coal, including pyritic sulfur, organic sulfur, and sulfate sulfur. This data is crucial for identifying the potential for sulfur gas emissions, such as SO_2, and determining the requirements for emission control systems in combustion processes. Unlike coal, natural gas was treated as a conventional mixture and defined directly from the component-wise molar composition of a natural-gas stream supplied to an Indonesian petrochemical plant. The composition used as the Aspen Plus feed input is presented in Table 4.

Table 1. Proximate Analysis of Feed Coal

Proximate Analysis	Value	Base
Moisture Content	4.9	% adb
Ash	9.2	% adb
Volatile Matter	45.7	% adb
Fixed Carbon	45.1	% adb

Table 2. Ultimate Analysis of Feed Coal

Ultimate Analysis	Value	Base
Ash	9.2	% adb
Carbon	67.1	% daf
Hydrogen	4.8	% daf
Nitrogen	1.1	% daf
Chlorine	0.1	% daf
Sulfur	1.3	% daf
Oxygen	16.4	% daf

Table 3. Sulfur Analysis of Feed Coal

Sulfur Analysis	Value	Base
Pyritic	0.6	% wt
Sulfate	0.1	% wt
Organic	0.6	% wt

Table 4. Molar composition of natural gas feed

Component Name	Molecule	%mol
Methane	CH_4	95.647
Ethane	C_2H_6	1.020
Propane	C_3H_8	0.367
Isobutane	C_4H_{10}	0.021
N-Pentane	C_5H_{12}	0.008
N-Hexane	C_6H_{14}	0.026
N-Butane	C_4H_{10}	0.082
Nitrogen	N_2	0.341
Carbon-Dioxide	CO_2	2.400

The natural-gas composition in Table 4 was obtained from the petrochemical company and represents the gas delivered to the plant boundary. The natural-gas heating value used in the simulation was 1006.866 Btu/scf. Sulfur-containing species, such as hydrogen sulfide, carbonyl sulfide, and mercaptans, were not reported in the available composition data and were therefore not included in the Aspen Plus model. This treatment should not be interpreted as confirmation that the natural gas contains zero sulfur. Gas absorption is commonly applied to remove acid gases such as H_2S and CO_2 from gas streams [4]. However, any upstream gas-sweetening or sulfur-removal process required to meet the delivered-gas specification was outside the system boundary of this study.

The fuel-characterization data presented in Tables 1–4 constitute the primary compositional inputs for reproducing the combustion models. Coal was defined using its proximate, ultimate, and sulfur analyses because it was treated as a non-conventional component in Aspen Plus. In contrast, natural gas was defined as a conventional mixture using its component-wise molar composition and heating value. These fuel specifications were subsequently combined with the operating conditions, thermodynamic methods, and reactor configurations summarized in Table 5.

2.2 Process Description

The coal- and natural-gas-fired furnace systems were modeled using Aspen Plus V14 to represent fuel combustion and hot-gas generation for the NPK fertilizer rotary dryer. The fuel properties and compositions reported in Tables 1–4 were used as the principal feed inputs for the respective combustion models. The two configurations were then developed using their corresponding thermodynamic methods, feed-flow bases, air-supply conditions, reactor models, operating conditions, and combustion reactions. To complement the fuel-characterization data and provide a reproducible simulation basis, the principal assumptions and model specifications applied to both configurations are summarized in Table 5.

Table 5. Aspen Plus simulation basis and technical differences

Parameters	Coal Furnace Simulation	Natural Gas Simulation
Fuel representation	Non-conventional solid defined by proximate, ultimate, and sulfur analyses	Conventional gas mixture defined by component-wise molar composition
Property Package	Peng-Robinson	Peng-Robinson
Reactor Model	RYield, RStoic, RCSTR	RCSTR
Operating Temperature (°C)	650 – 1200	1200 – 1600
Operating Pressure (bar)	1	0.975
Air Mass Flow (kg/hr)	5600	6566.7

Figure 1 presents the coal- and natural-gas-fired configurations within the same furnace–dryer system boundary. To preserve the visibility of unit operations and streams, the two wide Aspen Plus flowsheets are presented as a composite figure with vertically arranged panels. This format allows direct comparison of the fuel-handling, feed-preparation, and combustion sections while maintaining readability.

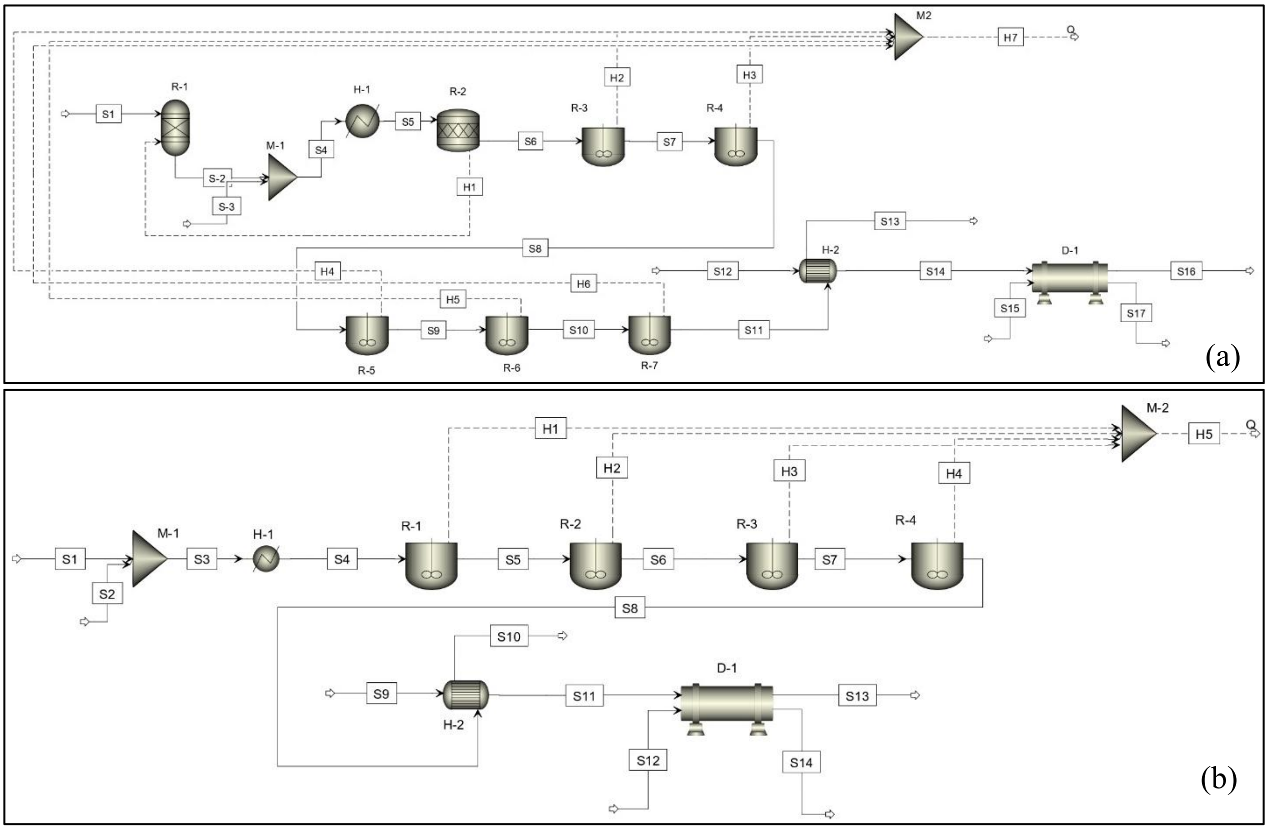

Figure 1. Comparative Aspen Plus flowsheets of the furnace–dryer system: (a) coal-fired configuration and (b) natural-gas-fired configuration.

2.2.1. Coal Furnace

The coal-fired configuration is shown in Figure 1(a). Coal was defined as a non-conventional component using the proximate, ultimate, and sulfur analyses reported in Tables 1–3. In RYield R-1, the coal was decomposed into conventional solid and gaseous species, including solid carbon, CO, CO_2, H_2, H_2O, CH_4, N_2, sulfur-containing species, and ash-related components. This approach enables the non-conventional coal feed to be represented in the subsequent stoichiometric and kinetic reaction blocks [17], [18].

The decomposition products were mixed with combustion air in Mixer M-1 and preheated in Exchanger H-1 before entering the combustion sequence. Oxidation of the volatile components was first represented in RStoic R-2 using the specified stoichiometric reactions. The remaining solid carbon and gaseous species were then oxidized in five sequential RCSTR blocks, R-3 through R-7, under steady-state and perfectly mixed conditions. The sequential reactor arrangement was used to represent changes in reaction progress, gas composition, and temperature along the modeled combustion section. The apparent Arrhenius power-law kinetics are described in Section 2.2.4 and Table 6 [18].

The resulting hot combustion gas was directed to HeatX H-2, where heat was transferred to the drying-air stream while maintaining physical separation between the combustion gas and the heated air. The heated air was subsequently supplied to rotary dryer D-1 for the NPK drying process. Energy streams associated with the decomposition, combustion, and heat-transfer blocks were used to determine the total heat generated and the useful heat transferred to the drying-air stream. The calculated heat output, direct CO_2 emission rate, and thermal efficiency were subsequently compared with the corresponding plant operating data in Section 3.1.

2.2.2. Natural Gas Furnace

The natural-gas-fired configuration is shown in Figure 1(b). Unlike coal, natural gas was represented as a conventional gaseous mixture using the component-wise molar composition reported in Table 4. Consequently, the natural-gas model did not require an RYield decomposition block or an RStoic conversion block. The natural-gas and combustion-air streams were combined in Mixer M-1 and preheated in Exchanger H-1 to the specified combustion-inlet condition before entering the reactor sequence.

Combustion was modeled using four sequential RCSTR blocks, R-1 through R-4, operated under steady-state, perfectly mixed conditions. The reaction set included complete and partial oxidation of methane and complete oxidation of the higher hydrocarbons present in the natural-gas feed. The use of simplified global reaction schemes for methane and higher alkane oxidation follows the approaches developed by previous studies [19], [20]. The apparent Arrhenius power-law kinetic expressions and corresponding parameters are presented in Section 2.2.4 and Table 7. The sequential reactor arrangement was used to represent changes in hydrocarbon conversion, combustion-product composition, and temperature throughout the modeled combustion section.

The hot combustion gas was subsequently directed to HeatX H-2 to transfer heat to the same drying-air stream and rotary dryer D-1 used in the coal configuration. This common downstream boundary enables the technical comparison to focus on differences in fuel handling, feed preparation, combustion configuration, and air demand. The compressor and gas-distribution piping were included in the equipment-cost boundary, although the natural-gas inlet pressure was specified directly in the Aspen Plus model rather than simulated using a separate compressor block. The calculated heat output, direct CO_2 emission rate, and thermal efficiency were evaluated against plant operating data in Section 3.1.

2.2.3. Technical Comparison of the Fuel Configurations

Figure 1 presents the coal- and natural-gas-fired configurations using a common furnace–dryer system boundary. Both configurations ultimately transfer the generated combustion heat through HeatX H-2 to the drying-air stream supplied to the same rotary dryer. Consequently, the principal technical differences occur in the fuel-handling, feed-preparation, and combustion sections rather than in the downstream drying process.

The coal configuration requires a solid-fuel conveyor and treats coal as a non-conventional component. Coal is initially decomposed in the RYield block, followed by stoichiometric conversion of the volatile products in RStoic and subsequent oxidation in the RCSTR sequence. This configuration must therefore represent devolatilization, solid-carbon oxidation, and ash-containing streams. In contrast, natural gas is introduced as a conventional gaseous mixture and does not require a decomposition block. The fuel is compressed, mixed with combustion air, preheated, and supplied directly to the RCSTR sequence.

Fuel switching consequently simplifies solid-fuel handling and eliminates the ash-forming feed from the combustion system, but requires a compressor and a dedicated gas-distribution and piping system. The two models also use different air-flow rates and combustion-temperature ranges. These changes affect the required equipment, installed capital cost, fuel and utility expenditure, direct CO_2 emissions, and thermal performance evaluated in the subsequent sections. Previous assessments of coal-fired industrial boilers have similarly shown that fuel-switching decisions involve trade-offs between fixed costs, operating costs, energy performance, and emissions [15]. The main technical differences are summarized in Table 5.

If sulfur compounds are present at concentrations requiring treatment at the plant, additional gas-cleaning or polishing equipment may be required; acid-gas absorption is one commonly applied treatment option [4]. Acidic service conditions can require dedicated corrosion-control measures for pipeline steels [21], while H_2S-containing sour environments can accelerate carbon-steel corrosion and require appropriate inhibition or material-protection strategies [22]. During combustion, H_2S and other sulfurous species may form SO_2 and related sulfur-containing products [12]. These additional requirements could increase installed capital cost, utility consumption, maintenance requirements, and annual operating expenditure. Because the concentrations and forms of sulfur compounds were unavailable, these effects were not quantified. The reported technical and economic results are therefore conditional on the delivered natural-gas specification presented in Table 4.

2.2.4. Reaction Kinetic Model

The reactions implemented in the RCSTR blocks were represented using an apparent Arrhenius power-law kinetic model. This common formulation was applied to both the coal-derived species and the natural-gas components to maintain consistency in the kinetic implementation. In the coal configuration, the RYield block first decomposed the non-conventional coal into conventional species, including solid carbon and volatile components. Consequently, oxidation of the resulting solid carbon was represented as a global power-law reaction between carbon and the gaseous reactants rather than through a separate particle-scale char-combustion submodel. The reaction rate for reaction j was calculated using Equation (1).

$$r_j = A_j T^{n_j} \exp\left(-\frac{E_{a,j}}{RT}\right) \prod_i C_i^{\alpha_{i,j}} \tag{1}$$

where r_j is the rate of reaction j, A_j is the pre-exponential factor, T is the reactor temperature in K, n_j is the temperature exponent, $E_{a,j}$ is the activation energy in $kJ.mol^{-1}$, R is the universal gas constant, C_i is the concentration of reactant i, and $\alpha_{i,j}$ is the corresponding reaction order. The apparent kinetic parameters were obtained from the supporting literature and entered into the Power Law reaction model in Aspen Plus. The concentration basis, reaction-rate basis, and units of the pre-exponential factor were defined consistently with the settings used in the simulation. The reaction-rate basis r_j was $kmol.m^{-3}.s^{-1}$, and reactant concentrations C_i were expressed in $kmol.m^{-3}$. The coal combustion reaction set includes oxidation of solid carbon, volatile components, carbon monoxide, hydrogen, and nitrogen-containing species. The corresponding reaction orders and Arrhenius parameters are summarized in Table 6. The natural-gas reaction set includes complete and partial oxidation of methane and the complete oxidation of the higher hydrocarbons present in the natural-gas feed, as summarized in Table 7.

Table 6. Power-law kinetic parameters for coal combustion reactions

Reaction (j)	$A_j, (s^{-1})$	n_j	$E_{a,j}, kJ.mol^{-1}$	**Reaction orders $\alpha_{i,j}$**	**Reference**
$C + O_2 \rightarrow CO_2$	4.53×10^2	0	1.495×10^3	O_2: 1	[23]
$CO + 0.5O_2 \rightarrow CO_2$	1.9×10^6	0	8.056	CO: 1 O_2: 0.3 H_2O: 0.5	
$CH_4 + 1.5O_2 \rightarrow CO + 2H_2O$	1.585×10^{10}	0	24.157	CH_4: 0.7 O_2: 0.8	
$H_2 + 0.5O_2 \rightarrow H_2O$	1.63×10^9	1.5	3.240	O_2: 1 H_2: 1.5	
$NH_3 + 1.25O_2 \rightarrow NO + 1.5H_2O$	3.38×10^7	0	10.000	NH_3: 1 O_2: 1	
$NH_3 + 0.75O_2 \rightarrow 0.5N_2 + 1.5H_2O$	3.38×10^7	0	10.000	NH_3: 1 O_2: 1	
$HCN + 0.75O_2 \rightarrow 0.5H_2 + CO + 0.5N_2O$	2.14×10^5	0	10.000	HCN: 1 O_2: 1	
$0.5N_2 + 0.5O_2 \rightarrow NO$	3×10^{14}	0	65.300	N_2: 1 O_2: 0.5	
$NO + C \rightarrow CO + 0.5N_2$	5.85×10^7	0	12.000	NO: 1	
$NO + CO \rightarrow CO_2 + 0.5N_2$	1.952×10^{10}	0	19.000	CO: 1	
$N_2O + C \rightarrow CO + N_2$	2.9×10^9	0	16.983	N_2O: 1	
$N_2O + CO \rightarrow CO_2 + N_2$	5.01×10^{13}	0	5.292	CO: 1 N_2O: 1	

Table 7. Power-law kinetic parameters for natural gas combustion reactions

Reaction (j)	$A_j, (s^{-1})$	n_j	$E_{a,j}, kJ.mol^{-1}$	**Reaction orders** $\alpha_{i,j}$	**Ref.**
$CH_4 + 0.5O_2 \rightarrow CO + 2H_2$	4.40×10^{11}	0	1.256×10^5	CH_4: 0.5 O_2: 1.25	[19]
$CH_4 + 1.5O_2 \rightarrow CO + 2H_2O$	1.585×10^{10}	0	24.157	CH_4: 0.7 O_2: 0.8	[23]
$CH_4 + 2O_2 \rightarrow CO_2 + 2H_2O$	1.3×10^8	0	202.506	CH_4: −0.3 O_2: 1.3	
$C_2H_6 + 3.5O_2 \rightarrow 2CO_2 + 3H_2O$	6.19×10^9	0	125.520	C_2H_6: 0.1 O_2: 1.65	
$C_3H_8 + 5O_2 \rightarrow 3CO_2 + 4H_2O$	4.84×10^9	0	125.520	C_3H_8: 0.1 O_2: 1.65	
$n - C_4H_{10} + 6.5O_2 \rightarrow 4CO_2 + 5H_2O$	4.16×10^9	0	125.520	$n - C_4H_{10}$: 0.15 O_2: 1.60	[20]
$n - C_5H_{12} + 8O_2 \rightarrow 5CO_2 + 6H_2O$	3.60×10^9	0	125.520	$n - C_5H_{12}$: 0.25 O_2: 1.50	
$n - C_6H_{14} + 9.5O_2 \rightarrow 6CO_2 + 7H_2O$	3.21×10^9	0	125.520	$n - C_6H_{14}$: 0.25 O_2: 1.50	

2.3 Process Evaluation Parameters

The dependent variables observed in this paper include CO_2 emissions generated from combustion processes using coal and natural gas, as well as techno-economic parameters such as Capital Expenditure, Operational Expenditure, NPV, IRR, and Payback Period. The independent variables used in this paper are the process configurations in the energy supply system for furnaces, specifically comparing the use of coal and natural gas.

2.3.1 Direct Combustion Emission Analysis

The environmental evaluation in this study was limited to direct emissions within the furnace system boundary. The boundary covers the fuel and combustion-air inputs and the resulting flue-gas outlet. Emissions associated with fuel extraction, processing, transportation, distribution, and fugitive methane leakage were not included. Accordingly, the calculated emissions represent onsite combustion emissions and should not be interpreted as a complete life-cycle carbon footprint. Fossil-fuel combustion is a major source of greenhouse-gas emissions and air pollutants [8]. Coal produces relatively high CO_2 emissions because of its high carbon content and may also generate sulfur oxides, particulates, ash, and unburned-carbon residues. In comparison, natural gas is predominantly composed of methane and has a higher hydrogen-to-carbon ratio, resulting in lower direct CO_2 emissions per unit of energy supplied. However, methane is itself a potent greenhouse gas. Therefore, the environmental benefit of switching to natural gas depends not only on its combustion-related CO_2 emissions but also on unburned methane at the furnace outlet and methane releases throughout the natural-gas supply chain [6].

Direct combustion emissions were evaluated using the CO_2 mass flow predicted by the Aspen Plus model and an emission-factor-based CO_2 estimate. The Aspen Plus result represents the process-specific CO_2 flow at the furnace outlet, whereas the emission-factor method provides an independent estimate based on the fuel energy input. The emission-factor-based direct CO_2 emission was calculated using Equation (2).

$$E_{CO_2,EF} = EF_{fuel}Q_{fuel} \tag{2}$$

where $E_{\mathrm{CO_2,EF}}$ is the emission-factor-based direct CO_2 emission rate, EF_{fuel} is the fuel-specific CO_2 emission factor, and Q_{fuel} is the fuel energy-input rate. Fossil-fuel combustion is a major source of greenhouse-gas emissions and air pollutants [8]. The emission factors adopted for sub-bituminous coal and natural gas were 96.1 and 56.1 kg CO_2/GJ, respectively [24], [25].

2.3.2 Techno-Economic Analysis

Capital expenditure (CAPEX) represents the initial investment required for combustion-system replacement. In this study, the installed capital cost within the selected project boundary was limited to the purchased cost of the furnace $(C_{furnace,j})$ and configuration-specific auxiliary equipment $(C_{aux,j})$, together with installation $(C_{installation,j})$ and piping costs $(C_{piping,j})$. Costs associated with new buildings, site development, utility-system expansion, control-system replacement, and working capital were excluded because the evaluation concerns modification of an existing operating facility. The installed CapEx of each configuration and the purchased furnace cost were calculated using Equations (3) and (4), respectively.

$$CAPEX_j = C_{furnace,j} + C_{aux,j} + C_{installation,j} + C_{piping,j} \tag{3}$$

$$C_e = a + bS^n \tag{4}$$

According to Towler and Sinnot, the furnace equipment cost can be estimated by its corresponding capacity, as suggested in Equation (4) [26]. Where C_e represents the cost of equipment purchased, both a and b are the cost constants, S is the size parameter, and n is the exponent for the type of equipment used. The constant and exponent values used in the equation may vary even when used for the same type of equipment. Each piece of equipment may have different technical specifications, such as operating pressure and temperature, material type, and additional designs or features that affect costs. In addition, differences in values can also arise because the data sources used to determine these parameters are not always consistent. This inconsistency depends on the cost estimation curve used, the regression method, and the range of equipment sizes at the time of data collection. So, even though the equipment generally looks similar, different technical details and calculation assumptions can cause the constant and exponent values to change. Meanwhile, the size parameter (S) value is obtained based on the design calculations from the technical specifications of the equipment used. This value represents the capacity or main dimensions of the equipment, which is used as a reference in determining the cost estimate.

After determining the price of the required equipment, it is adjusted to the CEPCI year used to update the price according to the year the equipment is used [27]. As shown in Equation (5), the updated cost of equipment in 2025, $C_{e,2025}$, is obtained by multiplying the equipment cost, $C_{e,ref}$, obtained in Equation (4) by the cost factor of comparison between CEPCI in 2025 and the CEPCI of the reference year associated with the cost correlation in Equation (4). Due to the unavailable data for CEPCI in 2025, the value is obtained through a linear regression approach based on historical CEPCI data for the year. The plot results produce a line equation, as shown in Equation (6), to project the CEPCI value for the analysis year.

$$C_{e,2025} = C_{e,ref}\ x\ \frac{CEPCI_{2025}}{CEPCI_{ref}} \tag{5}$$

$$CEPCI_y = 10.774y - 21133 \tag{6}$$

For this preliminary estimate, installation and piping costs were assumed to equal 25% and 15%, respectively, of the combined purchased cost of the furnace and configuration-specific auxiliary equipment, following a factorial cost-estimation approach [26]. Operational expenditure covers routine operational costs incurred, including direct and indirect costs such as fuel consumption, maintenance, and labor during the operational period. The amount is calculated based on the annual costs incurred during operation, using an approach shown in Equation (7).

$$OPEX_j = C_{direct,j} + C_{indirect,j} \tag{7}$$

where $OPEX_j$ is the annual operating expenditure of configuration j, while $C_{\mathrm{direct},j}$ and $C_{\mathrm{indirect},j}$ are its annual direct and indirect operating costs, respectively.

Direct costs include costs directly related to factory operations, such as fuel consumption, supporting raw materials, utilities (electricity, water, and steam), and direct labor. Indirect costs include maintenance, supervision, administration, and other operational overheads. Each cost component is calculated based on consumption rates, annual operating time, and respective unit prices to obtain an estimated annual OpEx used in the economic evaluation.

The financial evaluation was conducted on an incremental replacement, unlevered, and pre-corporate-income-tax basis using constant 2025 USD. Property-related taxes estimated as part of annual operating costs were retained, whereas corporate income-tax payments and depreciation tax benefits were excluded. The existing coal-fired furnace was assumed to require replacement at the beginning of the evaluation period; therefore, the natural-gas configuration was compared with a replacement coal-fired configuration. A project lifetime of 10 years and annual operating time of 7,920 h were adopted. A discount rate of 12% was selected as the base-case minimum required rate of return, consistent with the basis used in a previous process-economic assessment [28]. Financing costs, principal repayments, annual price escalation, and working capital were excluded. The incremental investment was calculated using Equation (8). The annual incremental cash flow consists of the difference in operating expenditure, which is calculated by Equation (9), and the assumed monetary benefit from the reduction in direct CO_2 emissions, as shown in Equation (10).

$$I_0 = CAPEX_{\mathrm{NG}} - CAPEX_{\mathrm{coal}} \tag{8}$$

$$\Delta OPEX = OPEX_{\mathrm{coal}} - OPEX_{\mathrm{NG}} \tag{9}$$

$$\Delta CF_t = \Delta OPEX + \Delta M_{\mathrm{CO_2}} P_{\mathrm{C}} \tag{10}$$

where I_0 is the incremental investment, $\Delta OPEX$ is the difference between annual coal and natural gas operating costs, ΔCF_t is the annual incremental cash flow, $\Delta M_{\mathrm{CO_2}}$ is the annual reduction in direct CO_2 emissions, P_{C} is the assumed carbon value. A positive $\Delta OPEX$ represents an operating-cost saving from fuel switching, whereas a negative value represents an increase in annual operating cost. The monetization of the direct CO_2 reduction was treated as a base-case scenario assumption. The calculation assumes that the complete direct emission reduction is eligible for monetization and that registration, monitoring, verification, and transaction costs are excluded. A carbon value of USD 12.84/tCO_2 was retained as a project-specific base-case assumption rather than an observed market price. This value lies within the low-to-moderate carbon-incentive range of USD 10–30/tCO_2 adopted in a previous scenario-based assessment of carbon-utilization projects [28].

For the final project year, the salvage value (SV) was added to the annual cash flow, as shown in Equation (11). The terminal salvage value was assumed to equal 10% of the purchased cost of the natural-gas furnace and was recognized as a cash inflow in year 10. No residual value was assigned to the compressor, piping, or installation costs.

$$\Delta CF_{10} = \Delta CF_t + SV \tag{11}$$

Net Present Value (NPV), calculated using Equation (12), represents the difference between the present value of future incremental cash flows and the initial incremental investment. A positive NPV indicates that the project creates economic value relative to the selected discount rate, whereas a negative NPV indicates that the discounted benefits are insufficient to recover the incremental investment.

$$NPV = -I_0 + \sum_{t=1}^{N} \frac{\Delta CF_t}{(1+r)^t} \tag{12}$$

where I_0 is the incremental investment, ΔCF_t is the incremental cash flow in year t, r is the discount rate, and N is the project lifetime.

The Internal Rate of Return (IRR), calculated using Equation (13), is the discount rate at which the project NPV equals zero. Under the selected decision criterion, the project is economically acceptable when its IRR exceeds the minimum required rate of return.

$$0 = -I_0 + \sum_{t=1}^{N} \frac{\Delta CF_t}{(1 + IRR)^t} \tag{13}$$

where I_0 is the incremental investment, ΔCF_t is the incremental cash flow in year t, IRR is the discount rate that produces an NPV of zero, and N is the project lifetime.

Because the IRR equation is nonlinear, the IRR value is generally determined using numerical methods, such as trial and error, interpolation, or spreadsheet software like Microsoft Excel. In this study, IRR was determined numerically using the Goal Seek function in Microsoft Excel. Meanwhile, the payback period, is calculated by Equation (14), indicates the time required to recover the initial investment based on the cash flow generated, thus serving as a benchmark for the speed of capital return.

$$PP = n + \left(\frac{a - b}{c}\right) \tag{14}$$

where n is the last complete year before investment recovery, a is the incremental investment, b is the cumulative cash flow through year n, and c is the cash flow occurring during year $n + 1$. The simple payback period was calculated using undiscounted incremental cash flows, whereas the discounted payback period was determined from cumulative cash flows discounted at 12%. This analysis aims to provide a comprehensive overview of whether switching from coal to natural gas as a fuel source is economically feasible, in line with increasing energy efficiency and reducing carbon emissions. The results of this analysis will serve as a basis for decision-making to assess the extent of fuel switching's impact on the sustainability and profitability of the production system.

3 Results and Discussion

3.1 Model Verification against Plant Data

The coal and natural gas combustion models were evaluated against operational data supplied by an Indonesian petrochemical company. The industrial dataset included heat output, CO_2 emission rate, and thermal efficiency for the corresponding coal and natural gas furnace configurations. Comparison of process-simulation outputs with measured combustion data has also been used to verify Aspen Plus coal-combustion models in previous studies [18]. Thermal efficiency was calculated using Equation (15), based on the ratio between the useful heat output and the energy supplied by the fuel:

$$\eta_{th} = \frac{net\ Q_{generated}}{\dot{m}_{fuel}.HV_{fuel}} \times 100\% \tag{15}$$

where η_{th} is the thermal efficiency, $net\ Q_{generated}$ is the heat transferred to the drying-air stream, $\dot{m}_{\mathrm{fuel}}$ is the fuel mass-flow rate, and HV_{fuel} is the heating value of the fuel. The values used for comparison represent nominal steady-state operating conditions at the air-supply rates, furnace temperatures, and pressures specified in Section 2.2 and Table 5. The representative plant values used for model comparison are reported in Tables 8 and 9. Accordingly, this evaluation verifies model consistency at the specified plant operating conditions rather than establishing predictive accuracy over the complete furnace operating range. The absolute relative error (ARE), defined in Equation (16), was calculated separately for each evaluated parameter.

$$Absolute\ Relative\ Error\ (ARE) = \left|\frac{Y_{sim} - Y_{plant}}{Y_{plant}}\right| \times 100\% \tag{16}$$

where Y_{sim} and Y_{plant} represent the simulation result and the corresponding plant value, respectively. Heat output, CO_2 emission rate, and thermal efficiency were assessed individually because they represent different physical quantities and have substantially different numerical scales. Combining them into a single aggregate error could obscure a relatively large deviation in one parameter.

The values used for comparison represent nominal steady-state operating conditions at the fuel flow rates, air-supply conditions, furnace temperatures, and pressures specified in Section 2.2 and Table 5. The aggregated plant values used for model comparison are reported in Tables 8 and 9. Accordingly, this evaluation is intended to verify model consistency at the specified plant operating conditions rather than establish predictive accuracy over the complete furnace operating range.

Table 8. Comparison of the Coal-Combustion Model with Plant Operating Data

Parameter	Simulation	Plant Data	ARE (%)
Heat Output, kW	4357.499	4357.500	0.000023
CO_2 Emission, kg/h	1297.41	1297.58	0.0131
Thermal Efficiency, %	89.91	76.00	18.30

Table 9. Comparison of the Natural-Gas-Combustion Model with Plant Operating Data

Parameter	Simulation	Plant Data	ARE (%)
Heat Output, kW	5789.639	5789.600	0.000674
CO_2 Emission, kg/h	940.456	940.560	0.0111
Thermal Efficiency, %	90.11	84.60	6.51

Tables 8 and 9 show that the predicted heat output and CO_2 emission rate closely agree with the corresponding plant data. For the coal configuration, the absolute relative errors for heat output and CO_2 emissions were 0.000023% and 0.0131%, respectively. For the natural-gas configuration, the corresponding errors were 0.000674% and 0.0111%. These results indicate that the principal heat-output and direct-emission predictions are numerically consistent with the selected plant operating data. A similar verification approach, involving comparison between Aspen Plus combustion-model outputs and measured data, has been reported by Liu et al. [18].

Greater deviations were observed for thermal efficiency. The coal model predicted a thermal efficiency of 89.91%, compared with the plant value of 76.00%, corresponding to an ARE of 18.30% and an absolute difference of 13.91 percentage points. The natural-gas model predicted 90.11%, compared with the plant value of 84.60%, resulting in an ARE of 6.51% and an absolute difference of 5.51 percentage points.

The larger deviation in the coal configuration may be attributed to steady-state model idealizations, including incomplete representation of furnace-wall radiation and convection losses, sensible heat carried by ash, incomplete combustion, and unburned-carbon losses. Differences between nominal model inputs and variable plant operation may also contribute to the deviation. Previous numerical studies have shown that coal-furnace predictions are influenced by combustion-air distribution and operating conditions, while detailed treatment of gas–solid behavior and combustion reactions affects agreement with measured data [7], [18]. Consequently, the models are considered suitable for comparing heat output and direct CO_2 emissions at the specified operating conditions, whereas their absolute thermal-efficiency predictions, particularly for coal combustion, should be interpreted cautiously.

Detailed information on measurement uncertainty and instrument calibration was unavailable for all variables because the operational dataset was supplied in aggregated form under industrial confidentiality restrictions. Therefore, measurement uncertainty could not be quantified or propagated through the model-verification calculations. Moreover, the available plant data were limited to the specified nominal operating conditions. Verification over broader variations in fuel flow, excess air, and furnace temperature, as well as a formal parametric sensitivity analysis, was therefore outside the scope of this study. The results should consequently be interpreted as a comparative model evaluation at the stated operating conditions rather than as evidence of predictive accuracy throughout the entire furnace operating envelope.

3.2 Direct Combustion Emission Results

Table 10 compares the direct CO_2 emission rates obtained from the Aspen Plus model and the corresponding emission-factor-based estimates. The Aspen Plus simulation predicted direct CO_2 emissions of 1.297 t/h for coal and 0.941 t/h for natural gas. Therefore, switching from coal to natural gas reduced the modeled onsite CO_2 emission rate by approximately 27.5%. The emission-factor method similarly produced lower direct emissions for natural gas, with estimates of 1.648 t CO_2/h for coal and 1.105 t CO_2/h for natural gas, corresponding to a reduction of approximately 33.0%. The difference between the two calculation methods arises because the Aspen Plus results account for the specific fuel composition and modeled combustion conditions, whereas the emission-factor method uses standardized fuel factors.

Table 10. Direct combustion emission indicators for coal and natural gas

Fuel	**Aspen-predicted CO_2 emission, t/h**	**Emission-factor-based direct CO_2 estimate, t/h**
Coal	1.297	1.648
Natural Gas	0.941	1.105

The Aspen Plus and emission-factor values represent two alternative calculation approaches and are not additive. The reported reductions apply only to direct furnace emissions. They do not include methane released during natural-gas production, processing, transmission, or distribution, nor fugitive emissions from valves, compressors, connections, and other components within the fuel-supply system. Combustion-related methane slip at the furnace outlet was also not separately assessed in the present environmental comparison. These sources can reduce the overall greenhouse-gas advantage of natural gas because methane has a substantially greater warming effect per unit mass than CO_2. Therefore, the 27.5% reduction should be interpreted as an onsite CO_2 reduction rather than a complete life-cycle greenhouse-gas reduction [6]. Ladage et al. showed that the climate benefit of coal-to-gas switching is strongly dependent on methane emissions throughout the natural-gas supply chain, although their case study concerns electricity generation rather than industrial process heating [29]. In addition, sulfur-related emissions were not evaluated because sulfur-containing species were not reported in the available natural-gas composition. If present, these species could contribute to SO_2 and other sulfur-containing combustion products, as discussed in Section 2.2.3 [12].

These results demonstrate the potential of fuel switching to reduce onsite combustion emissions from the NPK drying process. However, the net contribution to broader decarbonization targets would require a life-cycle assessment that includes the origin and transportation mode of the natural gas, supply-chain methane leakage, and fugitive emissions at the industrial facility. A complete life-cycle assessment was outside the scope of this study because site-specific data on natural-gas production, processing, transportation routes, and methane leakage rates were unavailable. Future assessments should incorporate these factors to determine whether the onsite CO_2 reduction is maintained across the complete fuel supply chain.

3.3 Techno-Economic Analysis

The calculated economic results are presented on the incremental replacement basis defined in Section 2.3.2. The analysis first compares the installed capital and annual operating costs of the replacement coal and natural-gas configurations. The resulting cost differences are then combined with the assumed monetary benefit of the direct CO_2 reduction to construct the incremental project cash flow. Economic feasibility is subsequently evaluated using NPV, IRR, simple payback period, discounted payback period, and carbon-value sensitivity.

In the initial stage of investment cost calculation, the Chemical Engineering Plant Cost Index (CEPCI) is used to calculate equipment prices from the reference year to the present year. The CEPCI value is used explicitly in estimating equipment costs in the chemical industry, a significant component in the capital expenditure calculation. The CEPCI-based cost escalation and factorial cost-estimation approach followed established process-design methods [26], [27]. The following CEPCI chart, shown in Figure 2, shows the trend in the index from 1996 to 2025.

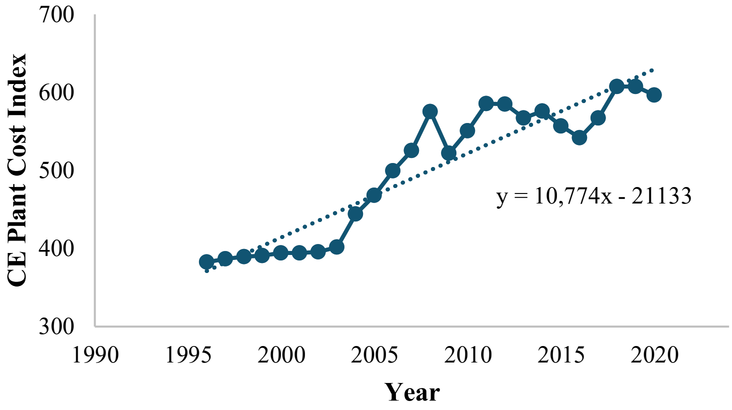

Figure 2. Historical CEPCI data from 1996–2020 and linear projection to 2025

The Chemical Engineering Plant Cost Index (CEPCI) was used to escalate reference equipment costs to the economic analysis year. CEPCI is commonly applied to adjust process-plant capital costs between different time periods [26], [27]. Because a consistent published annual value for 2025 was not available in the dataset used in this study, historical CEPCI values from 1996–2020 were fitted against calendar year using linear regression. Forecasting CEPCI from historical and economic trends has previously been investigated in process-cost estimation studies . The resulting correlation produced a projected 2025 CEPCI value of 684.35, which was used to escalate the reference equipment costs. Because the 2025 value was obtained through regression rather than from a published index, it should be interpreted as an estimated escalation factor [30]. The purchased-equipment, installation, and piping costs of the two replacement configurations are summarized in Table 11.

Table 11. Installed capital costs of the replacement configurations

Component	Coal, USD	Natural Gas, USD	Difference, USD
Furnace purchase cost	379,398.91	457,711.82	78,312.91
Compressor	-	11,281.82	11,281.82
Conveyor	38,080.32	-	-38,080.32
Installation	104,369.81	117,248.41	12,878.60
Piping	62,621.89	70,349.05	7,727.16
Total Installed CapEx	**584,470.93**	**656,591.10**	**72,120.17**

Table 11 shows total installed capital costs of USD 584,470.93 for the replacement coal configuration and USD 656,591.10 for the natural-gas configuration. Under the incremental replacement basis, the additional investment attributable to selecting natural gas is therefore USD 72,120.17. This amount represents the cost difference between the two replacement alternatives, rather than the full cost of constructing the natural-gas configuration. A terminal salvage value of USD 45,771.18, corresponding to 10% of the natural-gas furnace purchase cost, was included as a cash inflow in year 10. This value is included in the cash flow for the final year of the project as a positive component, which increases the Net Present Value (NPV) and strengthens the overall economic viability of the project. The estimated annual operating-cost components of the coal and natural-gas configurations are compared in Table 12.

The natural-gas configuration has an annual OpEx of USD 895,996.04, which is USD 12,594.33 higher than the coal-system OpEx of USD 883,401.71. Fuel expenditure increases by approximately 32.5% because of the assumed natural-gas price. This increase exceeds the savings obtained from lower utility, labor, maintenance, supervision, distribution, and supporting costs. Consequently, fuel switching does not provide a direct net operating-cost saving under the assumed prices, and the annual OpEx contribution to incremental cash flow is negative, valuing −12,594.33 USD/year. Although the natural-gas configuration has a higher annual OpEx, the base-case economic scenario includes the assumed monetary benefit associated with the reduction in direct CO_2 emissions.

Table 12. Annual operating costs of the coal and natural-gas configurations

Component	Coal, USD/year	Natural gas, USD/year	Difference, USD/year
Fuel	497,158.20	658,627.20	−161,469.00
Labor	42,217.93	35,646.45	6,571.48
Supervision	6,332.69	5,346.97	985.72
Utilities	212,286.55	109,990.74	102,295.81
Maintenance	29,223.55	13,131.82	16,091.73
Supporting raw materials	4,383.53	4,383.53	0
Laboratory	4,221.79	3,564.64	657.15
Insurance	5,844.71	6,565.91	−721.20
Property-related taxes	5,844.71	6,565.91	−721.20
Additional costs	46,664.50	32,475.14	14,189.36
Distribution	29,223.55	19,697.73	9,525.82
Operational Expenditure Total	**883,401.71**	**895,996.04**	**−12,594.33**

Table 13 presents the construction of the incremental cash flow used in the NPV, IRR, and payback calculations. The carbon-value benefit of USD 36,299.65/year exceeds the annual OpEx increase of USD 12,594.33/year, resulting in an annual net incremental cash flow of USD 23,705.32. The positive cash flow therefore arises from the assumed monetization of the direct CO_2 reduction rather than from an operating-cost saving. The cumulative discounted cash flow over the 10-year evaluation period is presented in Figure 3.

Table 13. Construction of the base-case incremental cash flow

Parameter	Value	Unit
Incremental investment	72,120.17	USD
Annual OpEx contribution	−12,594.33	USD/year
Direct CO_2 reduction rate	0.356954	tCO_2/h
Annual direct CO_2 reduction	2,827.08	$tCO_2/year$
Base-case carbon value	12.84	USD/tCO_2
Annual carbon-value benefit	36,299.65	USD/year
Annual incremental cash flow	**23,705.32**	**USD/year**
Terminal salvage value	45,771.18	USD
Year-10 cash flow	**69,476.50**	**USD**

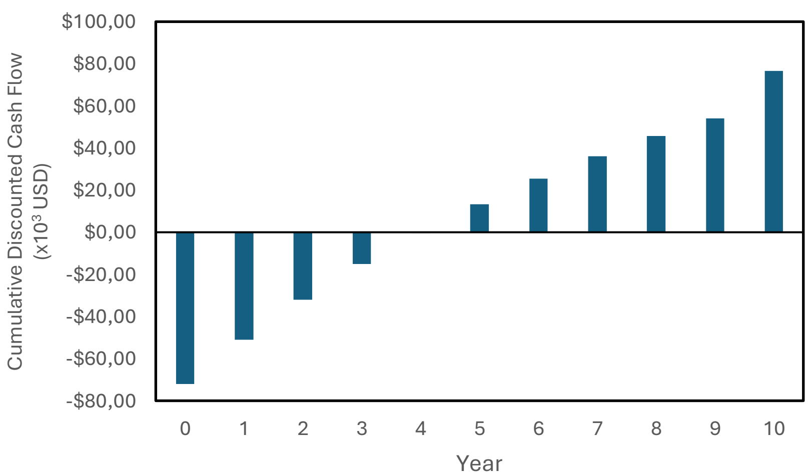

Figure 3. Cumulative discounted cash flow of the incremental fuel-switching project

The project begins with an incremental investment of USD 72,120.17 at year 0. At the 12% discount rate, cumulative discounted cash flow remains slightly negative at the end of year 4 and becomes positive early in year 5, corresponding to a discounted payback period of approximately 4.01 years. The simple payback period, calculated using undiscounted cash flows, is approximately 3.04 years. At the end of year 10, the cumulative discounted value reaches USD 76,557.28, corresponding to the project NPV. A positive NPV indicates that the incremental project creates economic value relative to the selected 12% discount rate [31]. The sensitivity of project NPV to the discount rate is presented in Figure 4.

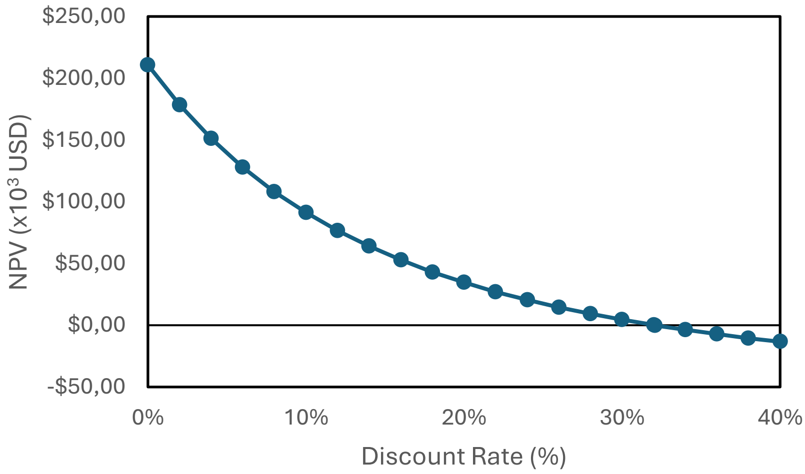

Figure 4. Sensitivity of project NPV to the discount rate

The project NPV decreases as the discount rate increases. At the selected discount rate of 12%, the project produces an NPV of USD 76,557.28. NPV reaches zero at approximately 32.10%, corresponding to the project IRR. Since the IRR exceeds the selected minimum required rate of return, the project satisfies the base-case economic criterion. Nevertheless, the economic conclusion is based primarily on NPV and supported by the IRR and payback indicators [31]. Because the annual incremental cash flow depends on monetization of the direct CO_2 reduction, the sensitivity of project NPV to the assumed carbon value is presented in Table 14.

Table 14. Sensitivity of NPV to the assumed carbon value

Scenario	**Carbon value, USD/tCO_2**	**NPV at 12%, USD**
No monetization	0.00	−128,543.85
Break-even carbon value	8.05	0.00
Low scenario	10.00	31,192.23
Base case	12.84	76,557.28

The results demonstrate that project feasibility is strongly dependent on the assumed monetary value of the CO_2 reduction. Without carbon monetization, the NPV decreases to −USD 128,543.85. The estimated break-even carbon value is approximately USD 8.05/tCO_2, below the base-case assumption of USD 12.84/tCO_2. Consequently, the project is economically feasible under the base case, but its attractiveness is conditional on the successful monetization of the direct emission reduction.

Overall, the natural-gas configuration requires a higher incremental capital investment and produces a slightly higher annual operating cost than the replacement coal configuration. Nevertheless, under the base-case assumptions, the assumed monetary benefit of the direct CO_2 reduction generates a positive incremental cash flow, NPV, and IRR. The economic result should therefore be interpreted as conditional on the incremental replacement boundary, the selected carbon value, and the assumed eligibility of the complete direct emission reduction for monetization. Fuel prices were held constant throughout the evaluation period; therefore, the reported economic indicators represent the stated base-case price conditions.

4 Conclusions

Based on the simulation and economic evaluation, switching from coal to natural gas provides technical and direct-emission benefits but is economically feasible only under the stated incremental replacement and carbon-value assumptions. At the furnace boundary, coal produced 1,297.41 kg CO_2/h, whereas natural gas produced 940.46 kg CO_2/h, corresponding to a 27.5% reduction in direct combustion emissions. This reduction excludes upstream and fugitive methane emissions and therefore does not represent a complete life-cycle greenhouse-gas benefit.

The natural-gas configuration requires an incremental investment of USD 72,120.17 and increases annual OpEx by USD 12,594.33 relative to the replacement coal configuration, primarily because of its higher fuel cost. Under the base-case carbon value of USD 12.84/tCO_2, the project yields an NPV of USD 76,557.28, an IRR of 32.10%, a simple payback period of 3.04 years, and a discounted payback period of 4.01 years. Without monetization of the direct CO_2 reduction, the NPV decreases to −USD 128,543.85. Consequently, the economic attractiveness of fuel switching is conditional on the incremental replacement boundary, the assumed carbon value, the eligibility of the direct emission reduction for monetization, and the base-case fuel prices.

Acknowledgment

This research was financially supported by the Final Project Assistance Grant (Bantuan Tugas Akhir Mahasiswa) funded by Institut Teknologi Sepuluh Nopember (ITS) under the 2025 ITS Internal Research Grant Scheme with the grant number 2110/PKS/ITS/2025 and Research Grant provided by DRPM ITS under the Penelitian Departemen with the grant number 2640/PKS/ITS/2025.

References

[1] S. Mingolla and L. Rosa, “Low-carbon ammonia production is essential for resilient and sustainable agriculture,” *Nat. Food*, vol. 6, no. 6, pp. 610–621, Feb. 2025, doi: 10.1038/s43016-025-01125-y.

[2] M. A. P. Kusuma, F. M. L. Sagala, T. D. Kusworo, and S. D. Laksono, “Performance Evaluation of Rotary Dryer and Granulator in NPK Steam Granulation Plant Production Department of IIB PT Petrokimia Gresik,” *Jurnal Global Ilmiah*, vol. 1, no. 5, pp. 287–302, Feb. 2024, doi: 10.55324/jgi.v1i5.44.

[3] V. Dwi Pratiwi, R. Handogo, R. P. Anugraha, J. Juwari, and R. Arifin, “Optimization of superstructure network in the CCS/CCSU system for CO2 reduction from exhaust gas industry and gas field in Indonesia as archipelago state,” *Chem. Eng. Commun.*, vol. 211, no. 9, pp. 1431–1444, 2024, doi: 10.1080/00986445.2024.2356829.

[4] R. Arifin, N. Faizah, A. I. Kaloka, A. F. Aulia, G. S. Thufailah, and M. A. Syukur, “Effect of Flow Rate NaOH on CO_2 Absorption Efficiency Using a Column Tray Absorber,” *IPTEK The Journal of Engineering*, vol. 11, no. 1, p. 22, Jun. 2025, doi: 10.12962/j23378557.v11i1.a22713.

[5] A. Deonarine, G. E. Schwartz, and L. S. Ruhl, “Environmental Impacts of Coal Combustion Residuals: Current Understanding and Future Perspectives,” *Environ. Sci. Technol.*, vol. 57, no. 5, pp. 1855–1869, Feb. 2023, doi: 10.1021/ACS.EST.2C06094.

[6] C. Gürsan and V. de Gooyert, “The systemic impact of a transition fuel: Does natural gas help or hinder the energy transition?,” *Renewable and Sustainable Energy Reviews*, vol. 138, p. 110552, Mar. 2021, doi: 10.1016/j.rser.2020.110552.

[7] S. Seputro and B. Sudarmanta, "Numerical Investigation of Over Fire Air (OFA) Effect on Flow Characteristics, NOx Combustion and Emission in a 600 Mw Tangentially Fired Pulverized Coal Boiler," *IPTEK The Journal of Engineering*, vol. 5, no. 2, pp. 38–42, May 2019, doi: 10.12962/j23378557.v5i2.a5017.

[8] M. Filonchyk and M. P. Peterson, "An integrated analysis of air pollution from US coal-fired power plants," *Geoscience Frontiers*, vol. 14, no. 2, p. 101498, Mar. 2023, doi: 10.1016/j.gsf.2022.101498.

[9] D. S. A. Suroso, B. Setiawan, P. Pradono, Z. S. Iskandar, and M. A. Hastari, "Revisiting the role of international climate finance (ICF) towards achieving the nationally determined contribution (NDC) target: A case study of the Indonesian energy sector," *Environ. Sci. Policy*, vol. 131, pp. 188–195, May 2022, doi: 10.1016/J.ENVSCI.2022.01.022.

[10] J. O. Robles, S. D. L. Almaraz, and C. Azzaro-Pantel, "Hydrogen Supply Chain Design: Key Technological Components and Sustainable Assessment," *Hydrogen Supply Chain: Design, Deployment and Operation*, pp. 37–79, Jan. 2018, doi: 10.1016/B978-0-12-811197-0.00002-6.

[11] J. A. Burney, "The downstream air pollution impacts of the transition from coal to natural gas in the United States," *Nat. Sustain.*, vol. 3, no. 2, pp. 152–160, Jan. 2020, doi: 10.1038/s41893-019-0453-5.

[12] A. Raj, S. Ibrahim, and A. Jagannath, "Combustion kinetics of H2S and other sulfurous species with relevance to industrial processes," *Prog. Energy Combust. Sci.*, vol. 80, p. 100848, Sep. 2020, doi: 10.1016/J.PECS.2020.100848.

[13] R. F. M. Zaky and D. A. Sari, "Upaya Pereduksian Emisi Karbon Dioksida (CO2) di Indonesia melalui Analisis Integrasi Power-to-Gas dengan PLTU Batubara," *SPROCKET JOURNAL OF MECHANICAL ENGINEERING*, vol. 5, no. 2, pp. 66–75, Feb. 2024, doi: 10.36655/sprocket.v5i2.1333.

[14] S. Koumi Ngoh, S. Epessé Missé, and I. Moungnutou Mfetoum, "Environmental and economic assessment of switching from heavy fuel oil to natural gas in industrial boilers and furnaces: Case of Cameroon, a low-income country," *Front. Energy Res.*, vol. 10, p. 1053576, Nov. 2022, doi: 10.3389/fenrg.2022.1053576.

[15] Y. Han, B. Shen, and T. Zhang, "A Techno-economic Assessment of Fuel Switching Options of Addressing Environmental Challenges of Coal-Fired Industrial Boilers: An analytical work for China," *Energy Procedia*, vol. 142, pp. 3083–3087, Dec. 2017, doi: 10.1016/J.EGYPRO.2017.12.448.

[16] S. K. Singal, V. Goel, H. Nautiyal, and D. E. Papantonis, "Economic and financial aspects of small hydropower," in *Small Hydropower*, Elsevier, 2023, pp. 245–257. doi: 10.1016/B978-0-323-91757-5.00001-4.

[17] J. Preciado, J. Ortiz-Martinez, J. Gonzalez-Rivera, R. Sierra-Ramirez, and G. Gordillo, "Simulation of Synthesis Gas Production from Steam Oxygen Gasification of Colombian Coal Using Aspen Plus®," *Energies (Basel).*, vol. 5, no. 12, pp. 4924–4940, Nov. 2012, doi: 10.3390/en5124924.

[18] B. Liu, X. Yang, W. Song, and W. Lin, "Process simulation of formation and emission of NO and N2O during coal decoupling combustion in a circulating fluidized bed combustor using Aspen Plus," *Chem. Eng. Sci.*, vol. 71, pp. 375–391, Mar. 2012, doi: 10.1016/j.ces.2011.10.050.

[19] W. P. Jones and R. P. Lindstedt, "Global reaction schemes for hydrocarbon combustion," *Combust. Flame*, vol. 73, no. 3, pp. 233–249, Sep. 1988, doi: 10.1016/0010-2180(88)90021-1.

[20] C. K. Westbrook and F. L. Dryer, "Simplified Reaction Mechanisms for the Oxidation of Hydrocarbon Fuels in Flames," *Combustion Science and Technology*, vol. 27, no. 1–2, pp. 31–43, Dec. 1981, doi: 10.1080/00102208108946970.

[21] L. A. Safitri, Y. T. Kuswanto, N. Husodo, E. Widiyono, H. Subiyanto, and D. M. Kusnadi, "Synergistic Temperature Effect on the Acid Corrosion Inhibition of API 5L Grade B Steel Using Eichhornia crassipes Leaf

Extract," *IPTEK The Journal of Engineering*, vol. 11, no. 3, p. 256, Dec. 2025, doi: 10.12962/j23378557.v11i3.a23162.

[22] M. Imran Ulhaq *et al.*, "Corrosion Inhibition of Carbon Steel in a Sour (H2S) Environment by an Acryloyl-Based Polymer," *ACS Omega*, vol. 8, no. 20, pp. 18047–18057, May 2023, doi: 10.1021/ACSOMEGA.3C01290.

[23] Z. Liu, W. Zhong, X. Liu, and Y. Shao, "Techno-economic and environmental evaluation of a supercritical CO2 coal-fired circulating fluidized bed boiler power generation," *Energy*, vol. 285, p. 129470, Dec. 2023, doi: 10.1016/J.ENERGY.2023.129470.

[24] S. Kim, J. Lee, S. Lee, C.-S. Cho, J.-H. Sa, and E.-C. Jeon, "Development of a CO2 emission factor in Korea from sub-bituminous coal by the classification method," *Environ. Earth Sci.*, vol. 72, no. 7, pp. 2325–2332, Oct. 2014, doi: 10.1007/s12665-014-3142-8.

[25] I. Bąk, A. Barwińska-Małajowicz, G. Wolska, P. Walawender, and P. Hydzik, "Is the European Union Making Progress on Energy Decarbonisation While Moving towards Sustainable Development?," *Energies (Basel).*, vol. 14, no. 13, p. 3792, Jun. 2021, doi: 10.3390/en14133792.

[26] G. Towler and R. A. Y. Sinnott, *Chemical Engineering Design*, vol. 2. Elsevier, 2022. doi: 10.1016/C2019-0-02025-0.

[27] R. P. Anugraha *et al.*, "Optimization of Process Economics in Mini Oil Refinery for Remote Areas," *Journal of Advanced Research in Fluid Mechanics and Thermal Sciences*, vol. 102, no. 1, pp. 14–24, Feb. 2023, doi: 10.37934/arfmts.102.1.1424.

[28] D. R. Zuchrillah *et al.*, "Comparison of Carbon Utilization Technologies for Decarbonization Strategy in the Ammonia Industry," *SINERGI*, vol. 30, no. 2, pp. 617–634, Jun. 2026, doi: 10.22441/sinergi.2026.2.024.

[29] S. Ladage, M. Blumenberg, D. Franke, A. Bahr, R. Lutz, and S. Schmidt, "On the climate benefit of a coal-to-gas shift in Germany's electric power sector," *Sci. Rep.*, vol. 11, no. 1, p. 11453, Jun. 2021, doi: 10.1038/s41598-021-90839-7.

[30] D. Mignard, "Correlating the chemical engineering plant cost index with macro-economic indicators," *Chemical Engineering Research and Design*, vol. 92, no. 2, pp. 285–294, Feb. 2014, doi: 10.1016/J.CHERD.2013.07.022.

[31] M. V. Sokolov, "NPV, IRR, PI, PP, and DPP: A unified view," *J. Math. Econ.*, vol. 114, p. 102992, Oct. 2024, doi: 10.1016/J.JMATECO.2024.102992.